DARK MATTER SEARCH WITH DEAP-3600 EXPERIMENT

Alexey Grobov (Kurchatov Institute)

for the DEAP Collaboration

NATIONAL RESEARCH CENTER "KURCHATOV INSTITUTE"

ICPPA-2020, MOSCOW

DEAP 3600

University of Alberta

AstroCeNT Nicolaus Copernicus Astronomical Center of the Polish Academy of Sciences

Canadian Nuclear Laboratories
Laboratoires Nucléaires Canadiens

Carleton University

Gobierno de España
Ministerio de Ciencia, Innovación y Universidades
Ciemat Centro de Investigaciones Energéticas, Medioambientales y Tecnológicas

TRIUMF

Technical University of Munich TUM

US University of Sussex

100+ researches in Canada, Germany, Italy, Mexico, Russia, Spain, UK, and USA

INFN Istituto Nazionale di Fisica Nucleare

Johannes Gutenberg Universität Mainz JG|U

National Research Center "Kurchatov Institute"

Laurentian University Université Laurentienne

iF Instituto de Física

SNOLAB

Particle Physics Rutherford Appleton Laboratory

Royal Holloway University of London

Queen's University

Princeton University

Dark matter detection principle

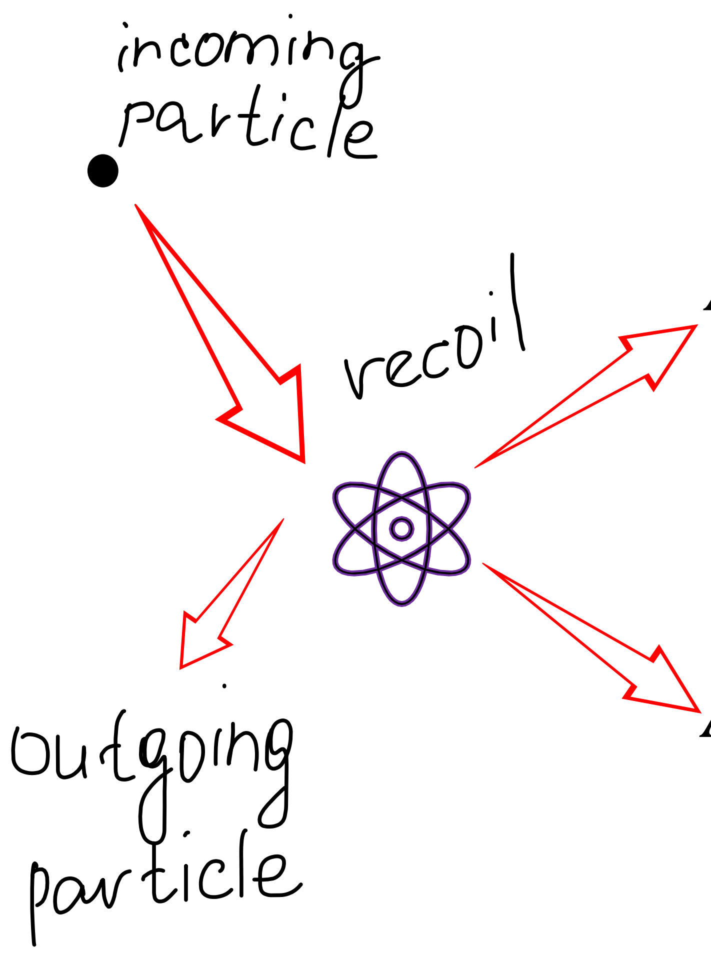

$$Ar^* + Ar \longrightarrow Ar_2^*$$

$$Ar^+ + Ar \longrightarrow Ar_2^+$$

$$e^- + Ar_2^+ \longrightarrow Ar_2^*$$

$$Ar_2^* \longrightarrow 2Ar + \underbrace{h\nu(128\,nm)}_{\text{UV light}}$$

SNOLAB
@SNOLABscience

Hunt for the unseen
A whir, bubble, flash of light
Dark matter escapes

📷 Aric Guite, Robert Provencher, Douglas Takayesu

The DEAP Collaboration, *Design and Construction of the DEAP-3600 Dark Matter Detector*, Astropart. Phys. 108, 1 (2019).

DEAP-3600 detector

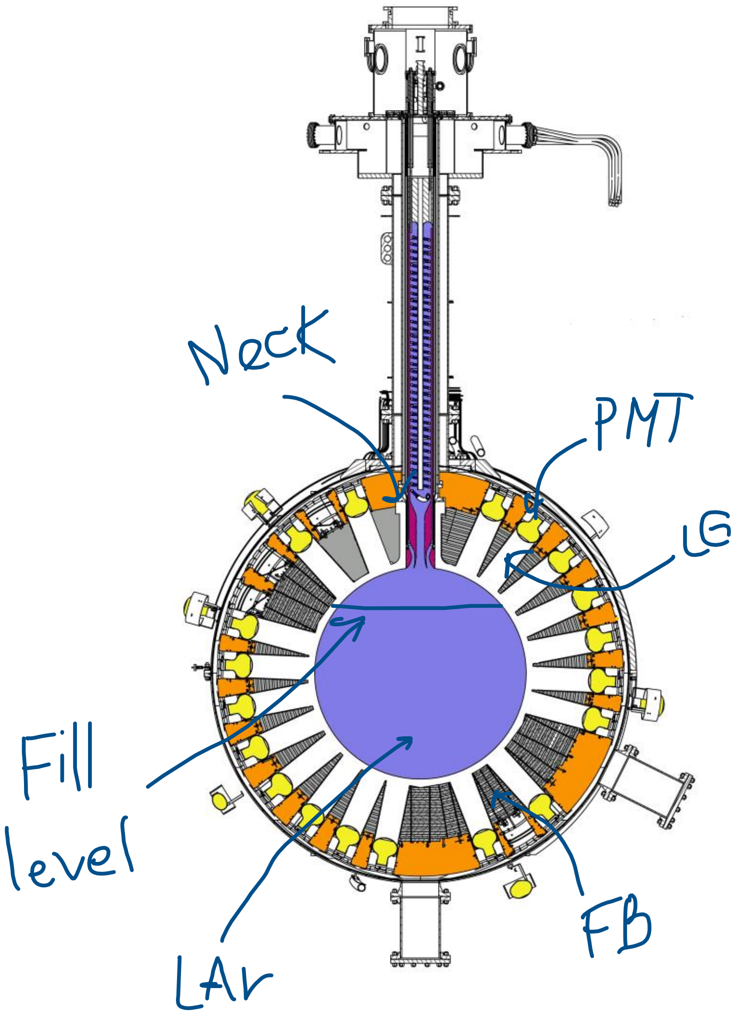

DEAP-3600 is a single-phase liquid argon (LAr) direct-detection dark matter experiment.

Location: 2km underground at SNOLAB (Sudbury, Canada).

Target: 3279 kg of LAr (30 cm of GAr on top) in a spherical acrylic vessel (AV)

Light detection: 255 PMTs connected to AV by 45 cm light guides (LGs).

Construction: Filling of the detector done through the neck with LN2 cooling coil.
AV and PMTs enclosed in stainless steel shell.

Shielding: Filler blocks between LGs used for thermal insulation and neutron shielding.
Steel shell is immersed in 300 tons of H_2O, viewed by 48 veto PMTs.
Neck of the detector has 4 Neck veto PMTs.

Photoelectron counting and PSD parameter

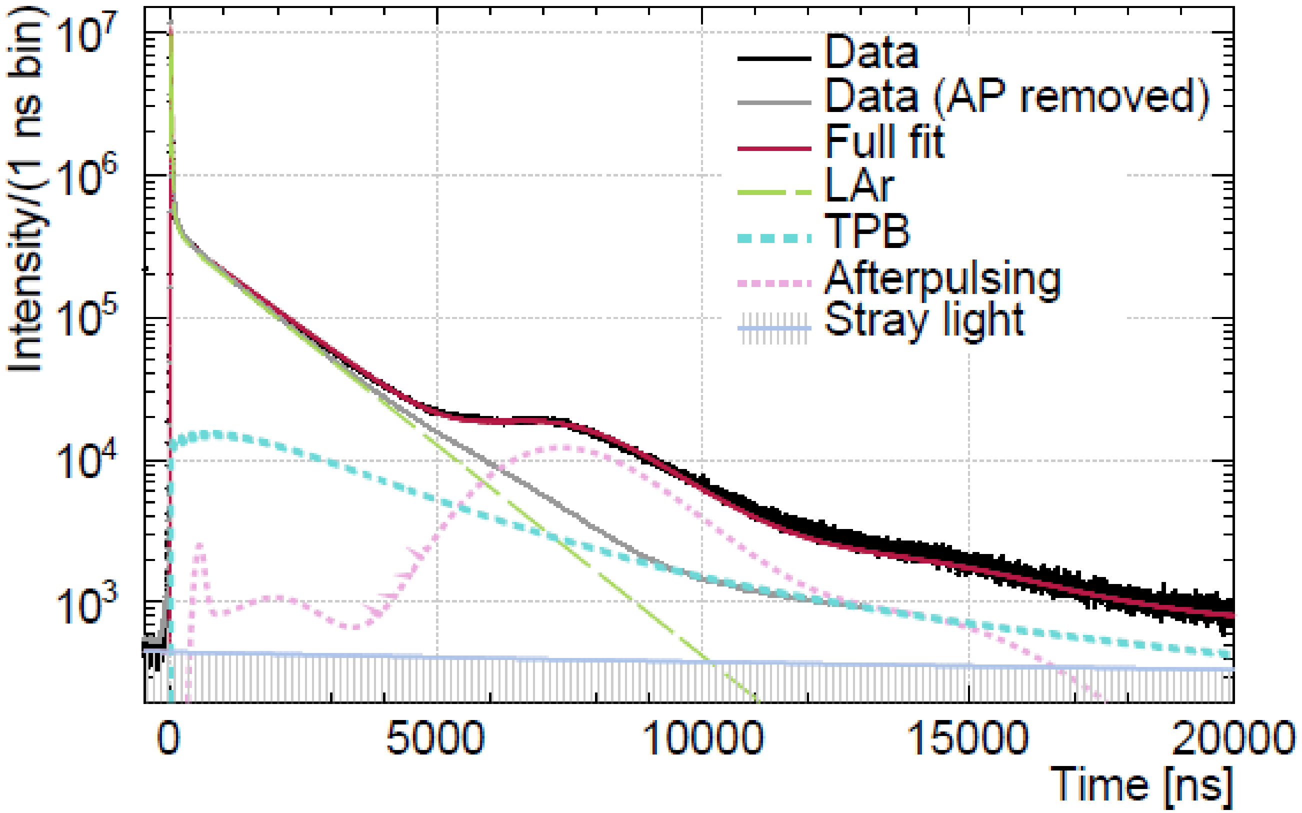

Ar39 pulseshape and model fit incorporating several components. Ar39 beta-decays with lifetime ~269 years. It is a source of electron recoils in LAr.

Excited argon dimers can be either singlet or triplet states, which have different decay time (7ns and 1.3μs). Depending in type of the recoil (electron or nuclear) there will be different ration of singlet to triplet states.

This allows to distinguish between nuclear and electron recoils by shape of the scintillation pulse.

$$F_{\text{prompt}} = \frac{\sum_{t=-28\,\text{ns}}^{60\,\text{ns}} \text{PE}(t)}{\sum_{t=-28\,\text{ns}}^{10\,\mu\text{s}} \text{PE}(t)}$$

Fprompt distibutions

Electron recoils

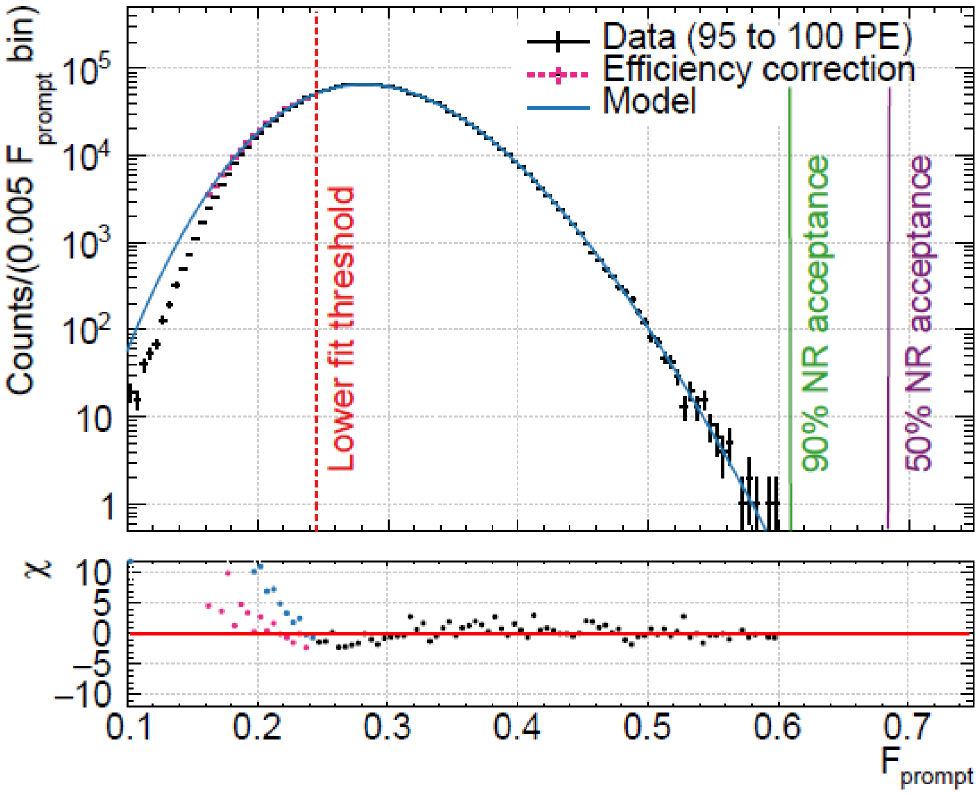

Fprompt distribution for ERs from standard physics data in the lowest 1 keVee energy bin in the WIMP-search ROI.

Nuclear recoils

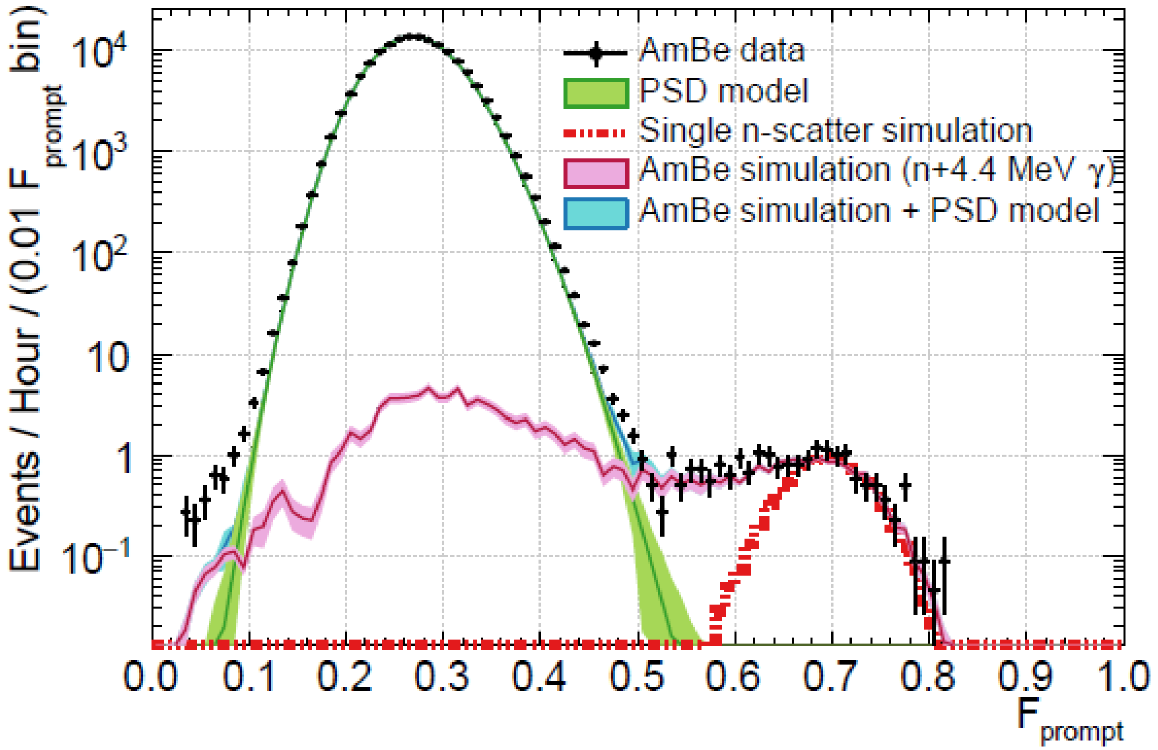

Using AmBe calibration to validate PSD

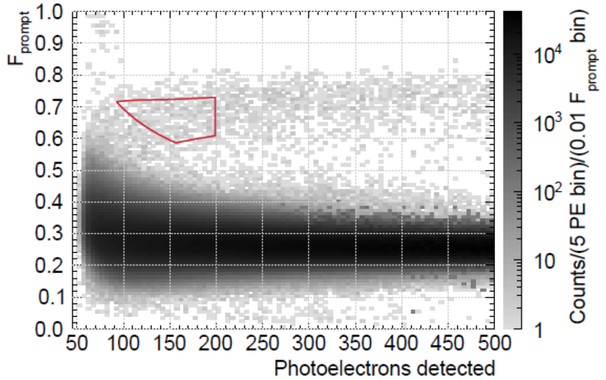

Efficiency correction is described in Eur. Phys. J. C (2019) 79: 322

Response calibration & energy reconstruction

Alpha decays in LAr bulk

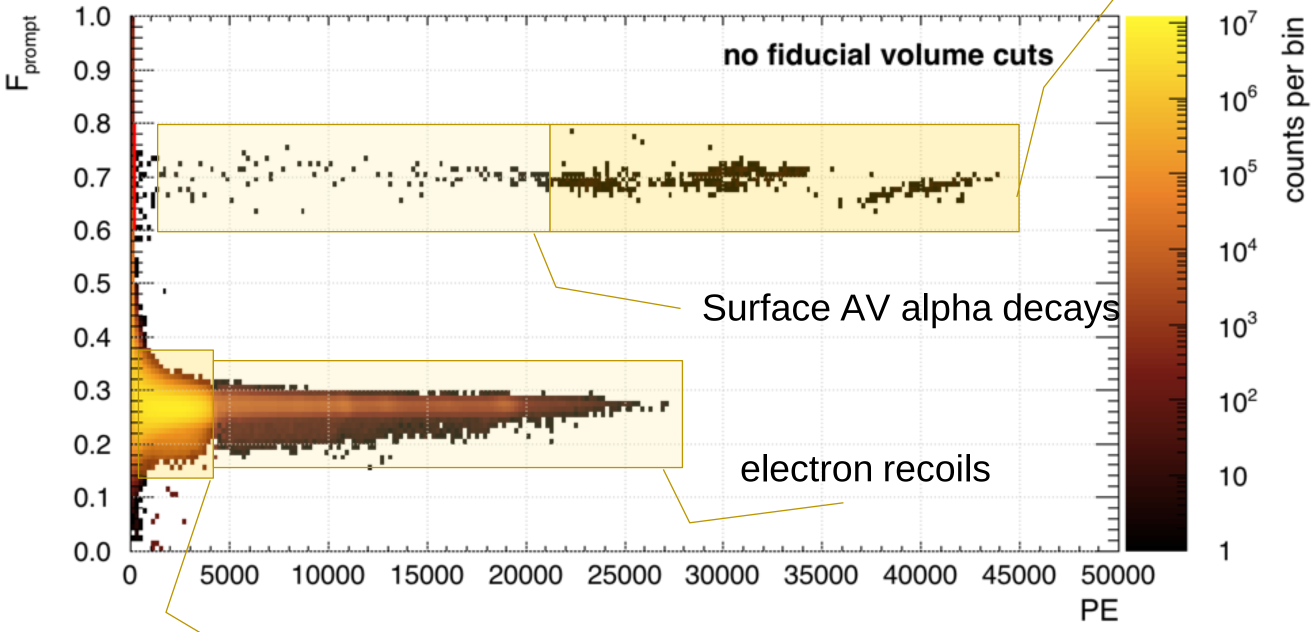

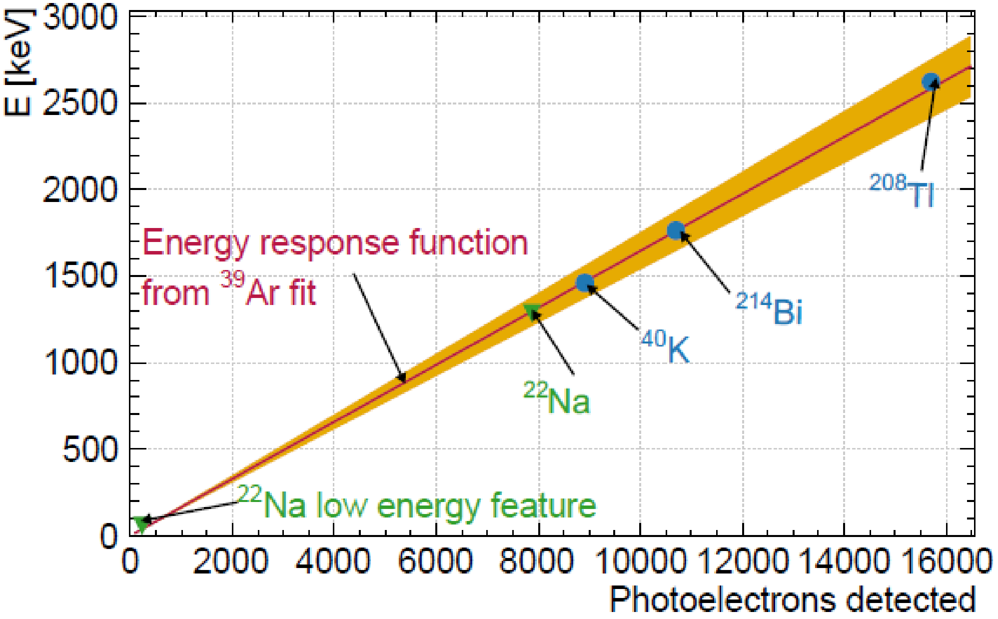

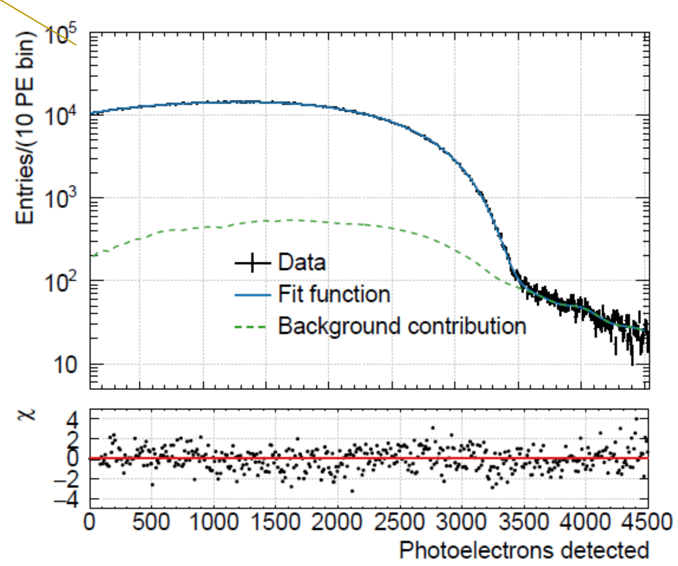

Ar39 model fit to data.

Energy response function, showing the number of detected photoelectrons versus energy deposited in LAr by event.

Position reconstruction

DEAP-3600 utilizes two complementary position reconstruction algorithms

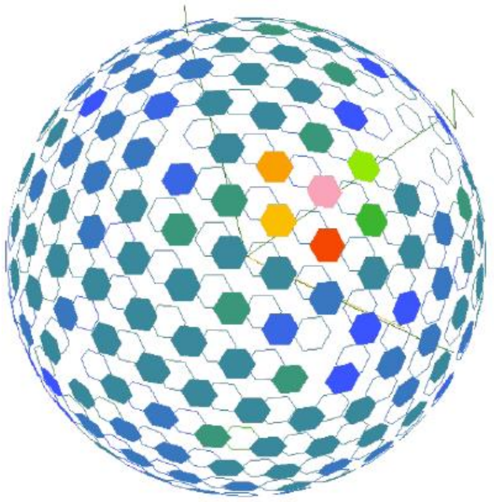

spatial distribution of PMT hits (PE-based algorithm)

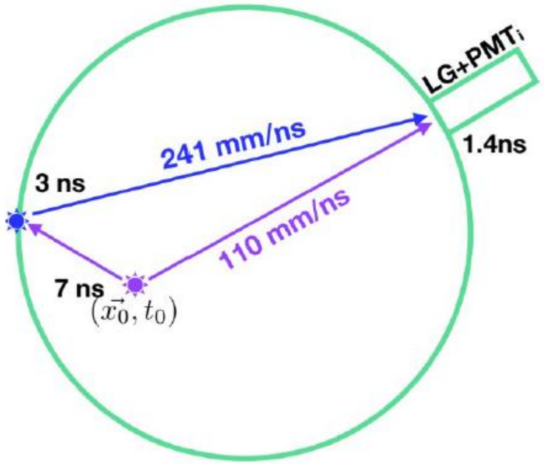

time residual based algorithm

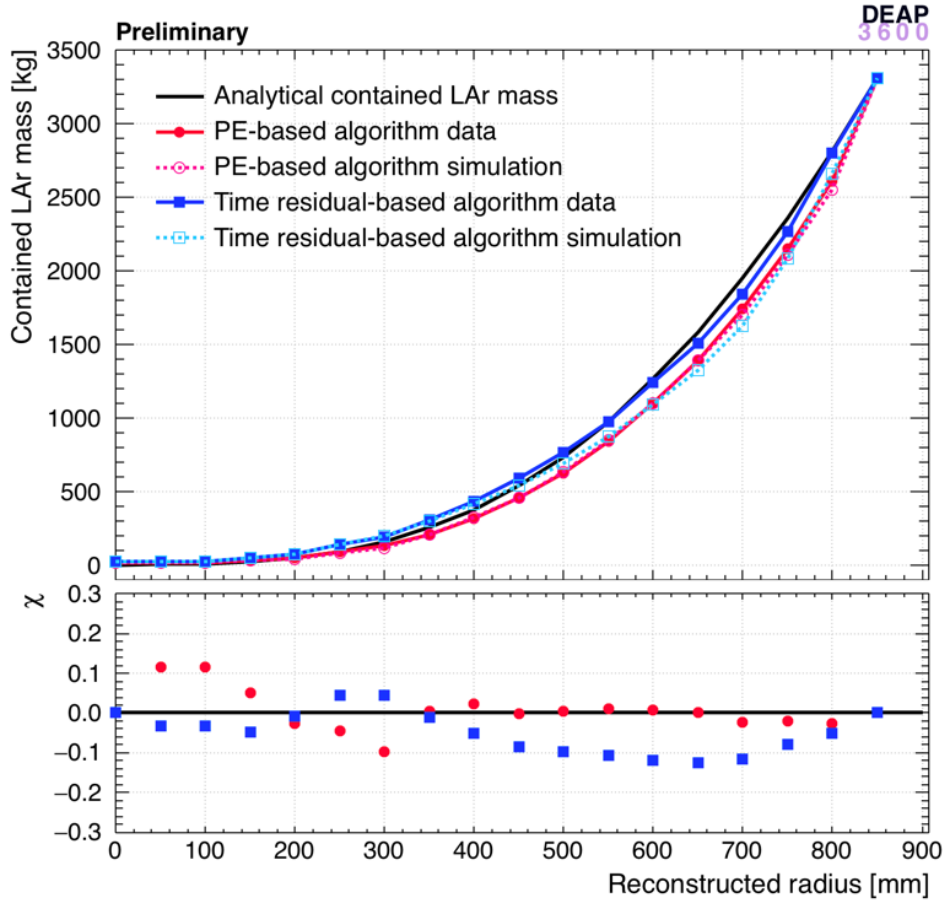

Estimates from the PE-based (red) and time residual-based (blue) algorithms of the contained mass of LAr within a radius of the reconstructed position.

Backgrounds model: components and approach

- Cosmogenic neutrons
- Radiogenic neutrons
- Cherenkov light
- Alpha-decays
- Ar39 component
- Other possible backgrounds?

- Using MC simulations, sidebands and calibration to develop the model
- Validate it on control regions in data
- Develop event selection based on background model
- Predict number of events in ROI

	Source	N^{CR}	$N^{\mathrm{ROI,\ LL}}$	N^{ROI}
β/γ's	ERs	2.44×10^9	0.34 ± 0.11	0.03 ± 0.01
	Cherenkov	$< 3.3 \times 10^5$	< 3890	< 0.14
n's	Radiogenic	6 ± 4	11^{+8}_{-9}	$0.10^{+0.10}_{-0.09}$
	Cosmogenic	<0.2	<0.2	<0.11
α's	AV surface	<3600	< 3000	< 0.08
	AV Neck FG	28^{+13}_{-10}	28^{+13}_{-10}	$0.49^{+0.27}_{-0.26}$
	Total	N/A	< 4910	$0.62^{+0.31}_{-0.28}$

Neutrons

Cosmogenic

Cosmogenic neutrons are produced by high energy atmospheric muon interactions with the detector and its environment

- Muons are tagged when passing through muon veto

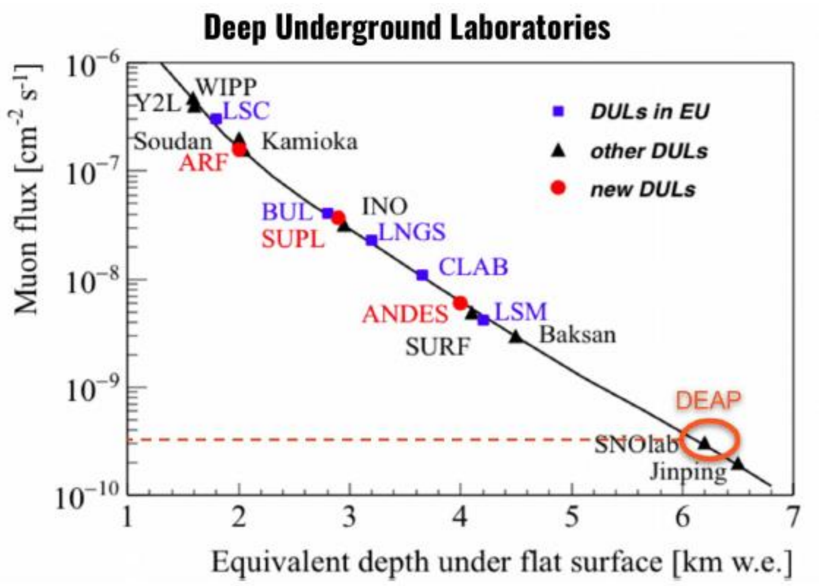

Radiogenic

Radiogenic neutrons can be produced in the (α,n) reaction triggered by α-decays from Uranium/Thorium chains or by the spontaneous fission of 238U.

Main source of neutrons – PMT Glass. Neutron rate is reduced by the passive shielding.

Mitigation is done by:

- Estimation of flux with material assays
- Neutron capture analysis: tagging NR event closely followed (1ms) by high energy ER event

P.-A. Amaudruz et al. (DEAP-3600 Collaboration), Astropart. Phys. 108, 1 (2019).

Beta particles and gamma rays

Ar39 beta-decays

- Main source of ERs
- Have low Fprompt values

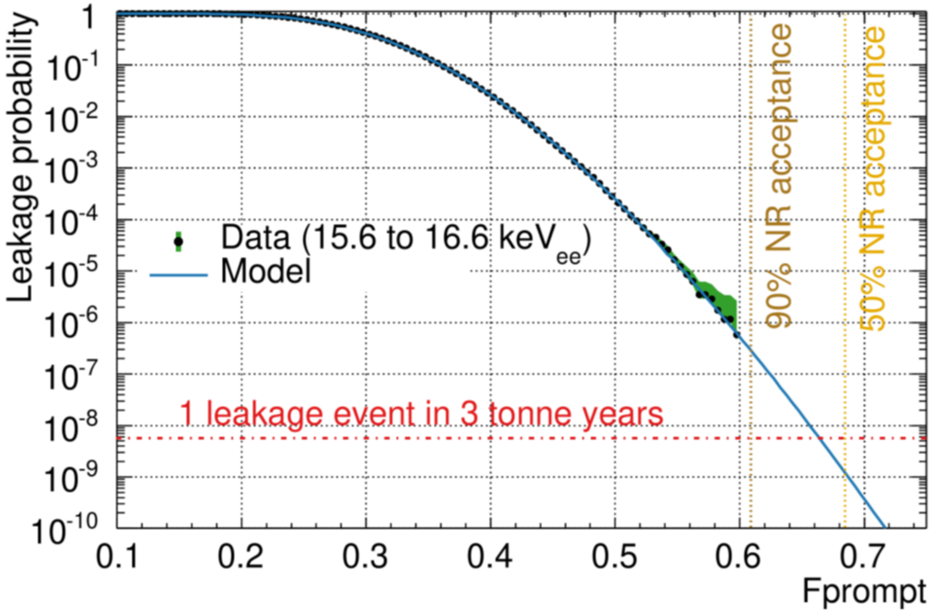

Cherenkov light

- Produced in the acrylic or PMT glass
- Have high Fprompt values
- Calibrated with U232 source
- mitigated by removing events with more than 40% of the total event charge in one PMT
- Fiducial radius cut removes dffuse light

Alpha decays: Surface AV

Mostly Po210 decays (daughter of Pb210 from U238 progeny)

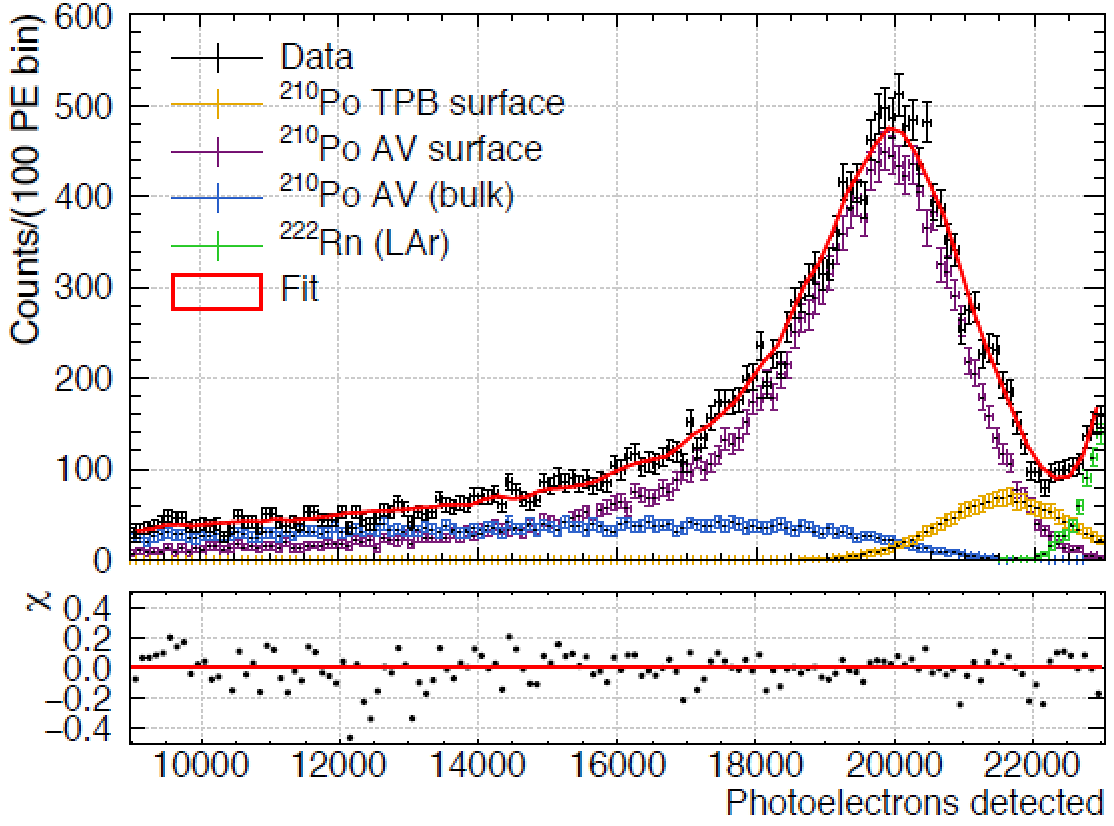

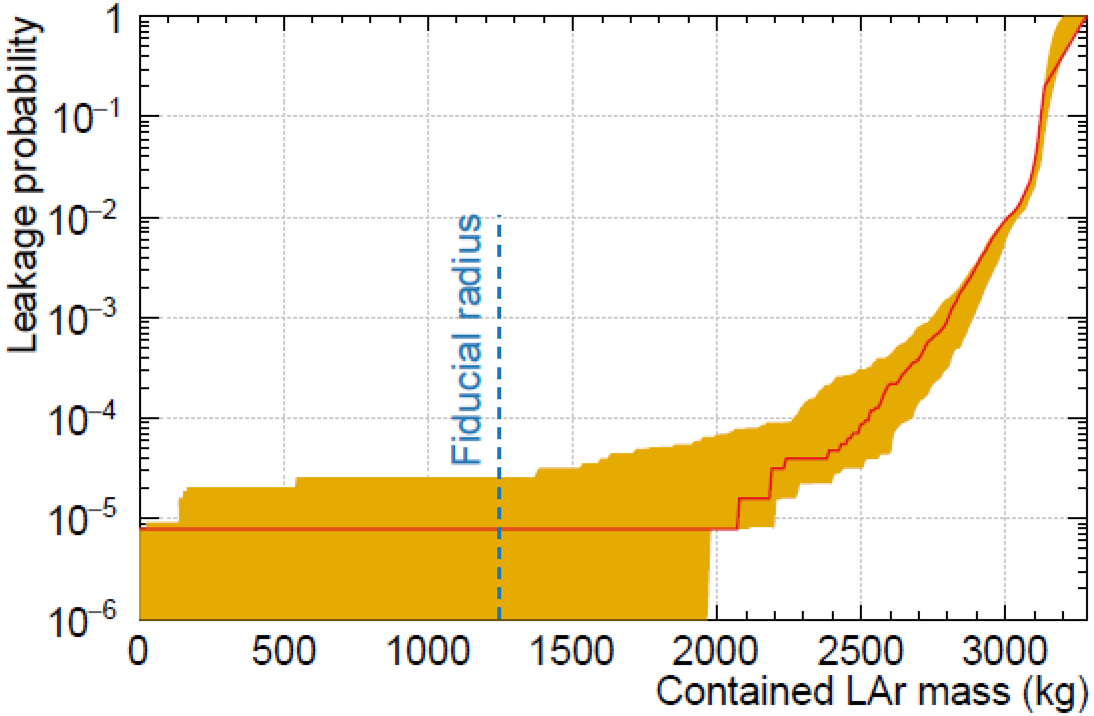

Alpha decays: Neck

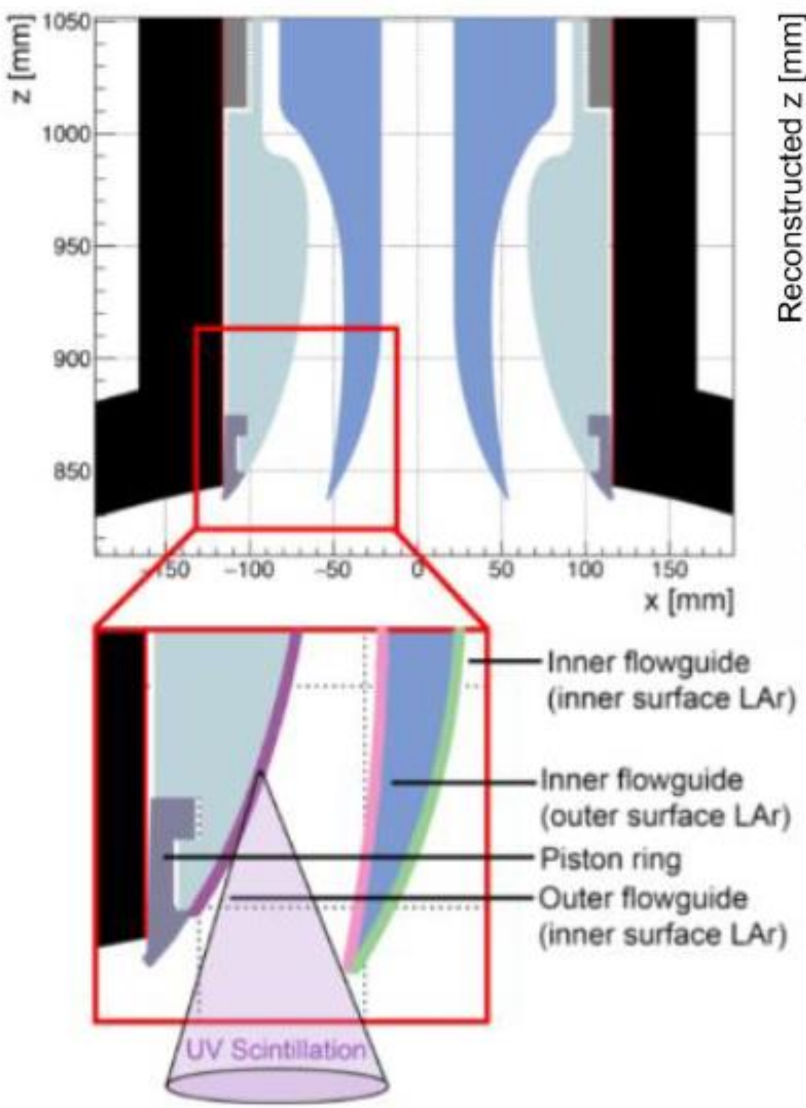

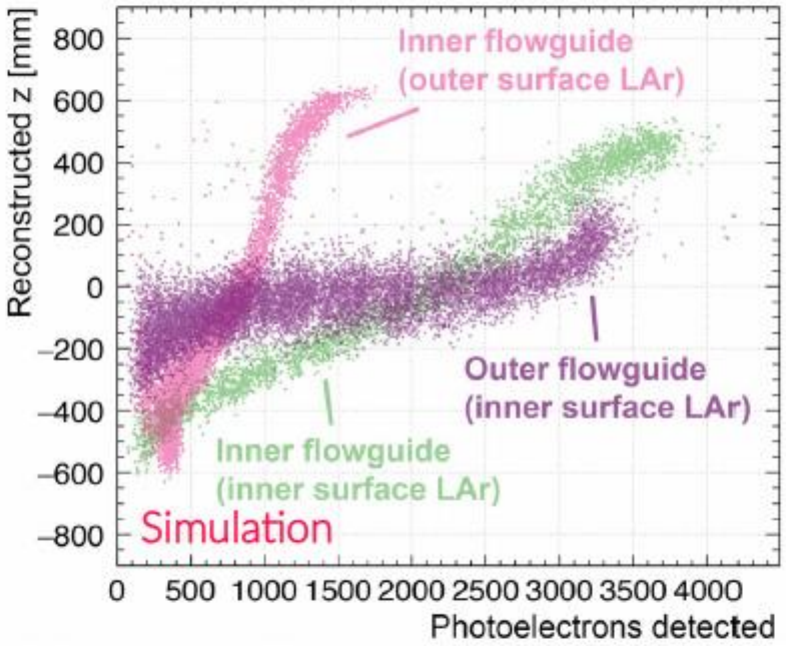

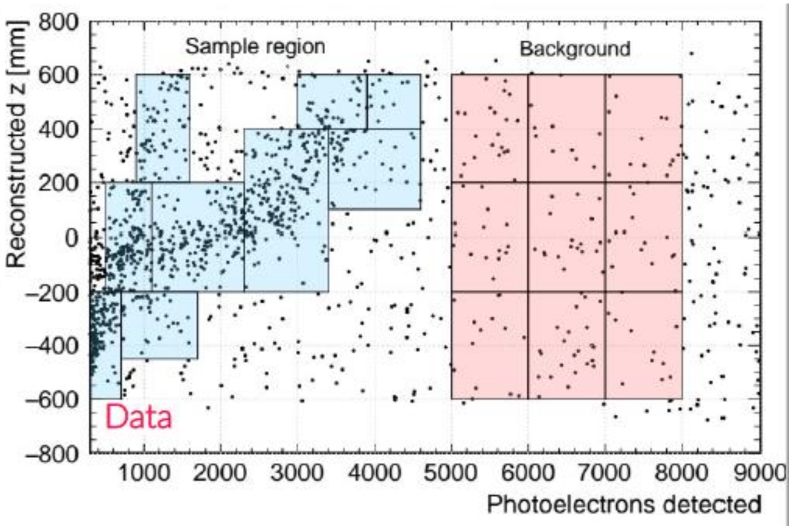

Most crucial background component

Rates:
Inner flowguide, inner surface: 14.1 μHz
Inner flowguide, outer surface: 16.8 μHz
Outer flowguide, inner surface : 22.7 μHz

This background is mitigated with:

- Accounting for early pulses in GAr PMTs
- Upper Fprompt cut
- Charge fraction in top 2 rows of PMTs
- neck veto PMTs
- Position reconstruction consistency

ROI definition and Acceptance

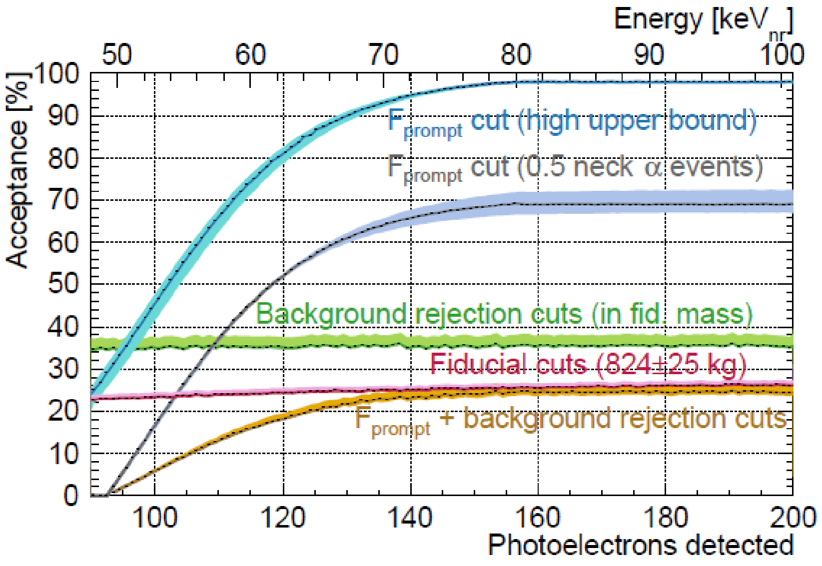

	Background rejection cut	WIMP accept. [%]	$N_{\rm bkg}^{\rm ROI}$	$N_{\rm obs}^{\rm ROI}$
Cherenkov	Neck veto	$92.0^{+1.0}_{-0.1}$	$9.2^{+4.4}_{-3.5}$	29
α-decays in neck	Early pulses in GAr PMTs	$45.4^{+1.5}_{-0.1}$	$2.3^{+1.1}_{-0.9}$	2
	Position fitter consistency	$35.4^{+2.5}_{-0.1}$	$0.62^{+0.31}_{-0.28}$	0
	Total	$35.4^{+2.5}_{-0.1}$	$0.62^{+0.31}_{-0.28}$	0

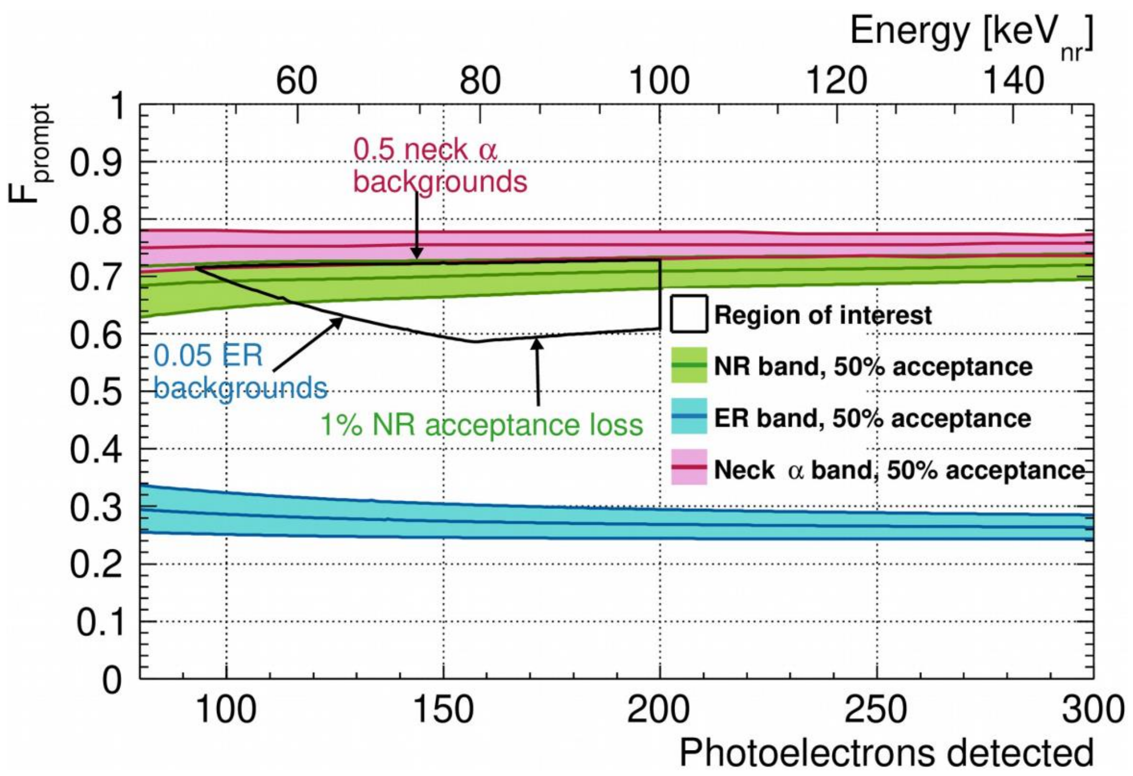

WIMP ROI (black) along with the ER (blue), NR (green) and neck -decay (pink) bands that define the boundaries

WIMP search results

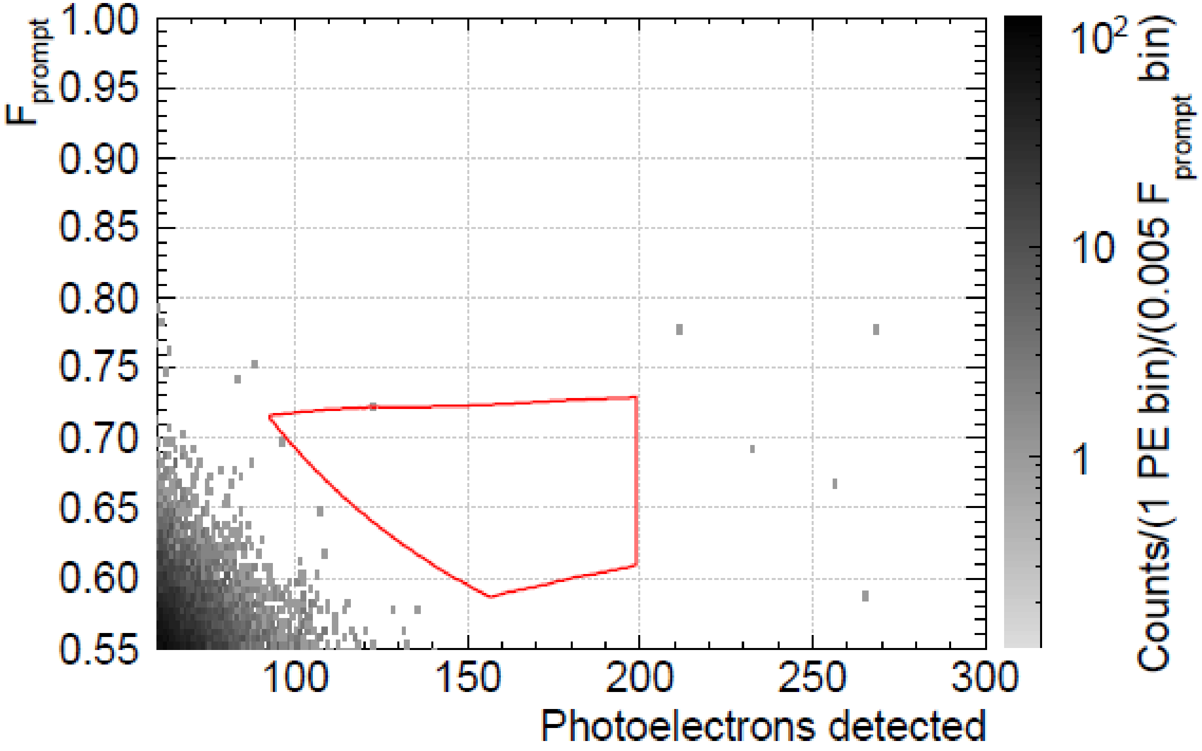

No events remained in the ROI after all cuts

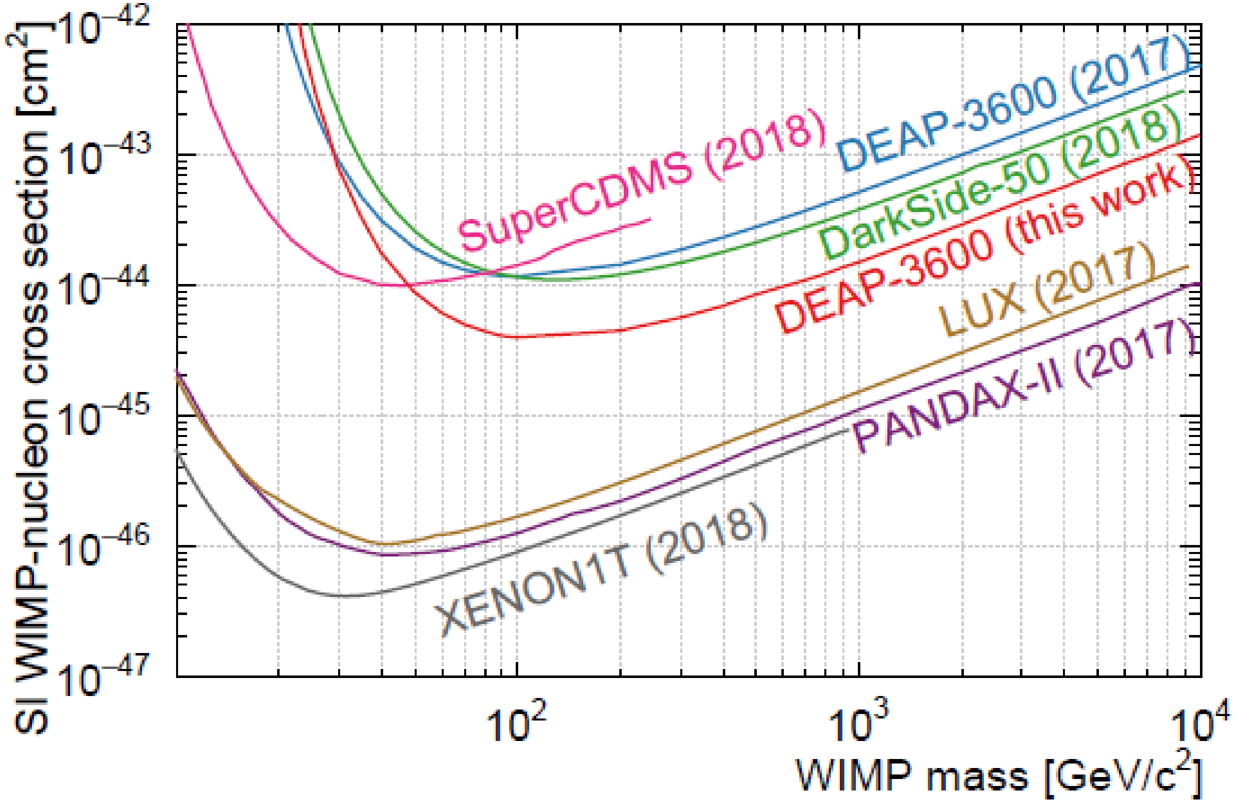

90% condence upper limit on the spin-independent WIMP-nucleon cross sections

Exclude cross sections above 3.9×10-45 cm2 (1.5×10-44 cm2) for 100 GeV/c2 (1 TeV/c2) WIMP mass

Constraints on EFT models

Astrophysics model

$$\boxed{\frac{dR}{dE_R}} = \boxed{\frac{\rho_T}{m_T}} \cdot \frac{\boxed{\rho_\chi}}{\boxed{m_\chi}} \boxed{\epsilon(E_R)} \int_{v_{\{min\}}}^{\infty} \boxed{v f_\chi^{\oplus}(\vec{v})} \boxed{\frac{d\sigma}{dE_R}} d^3\vec{v}$$

Diff. scat. rate

Detector model

Particle physics model

Constraints on dark matter-nucleon effective couplings in the presence of kinematically distinct halo substructures using the DEAP-3600 detector, 2005.14667

Particle physics model

$$L_{int} = \sum_{n,p} \sum_{i} c_i^{(N)} \mathcal{O}_i \chi^+ \chi^- N^+ N^-$$

$$\mathcal{O}_1 = 1_\chi 1_N$$

$$\mathcal{O}_3 = i\vec{S}_N \cdot \left(\frac{\vec{q}}{2m_N} \times \vec{v}_\perp\right)$$

$$\mathcal{O}_5 = i\vec{S}_\chi \cdot \left(\frac{\vec{q}}{2m_N} \times \vec{v}_\perp\right)$$

$$\mathcal{O}_8 = \vec{S}_\chi \cdot \vec{v}_\perp$$

$$\mathcal{O}_{11} = \vec{S}_\chi \cdot \frac{\vec{q}}{2m_N}$$

Fan et al. (2010), Fitzpatrick et al. (2013)

Astrophysics model

$$f_\chi^{\{gal\}}(\vec{v}) = (1 - \eta_{sub}) f_{SHM}^{\{gal\}}(\vec{v}) + \eta_{sub}\, f_{sub}^{\{gal\}}(\vec{v})$$

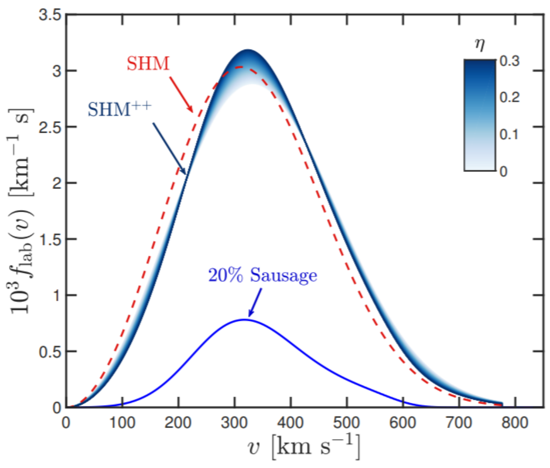

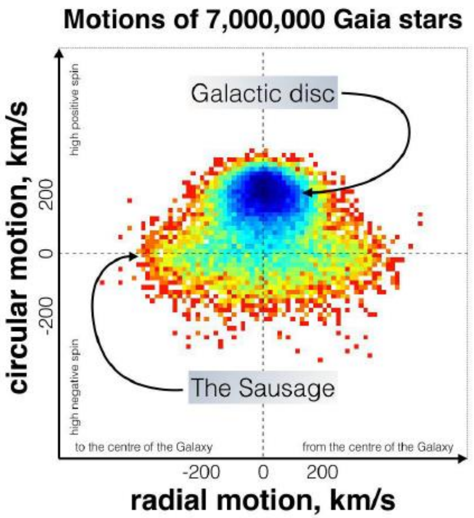

Types of Substructures:

- Gaia Sausage (Necib et al.)
- Gaia Sausage (O'Hare et al.) O'Hare *et al.* Phys. Rev. D 98, 103006 (2018)
- G1: Koppelman 1
- G2: Koppelman 2 H. Koppelman et al., Astrophys. J. 860, L11 (2018)
- G3, G4: IC (In-falling clumps)
- G5: Helmi H. Koppelman *et al.* Astron. Astrophys. 625, A5 (2019)
- G6: Nyx L. Necib *et al.*, arXiv:1907.07190

Constraints on EFT models

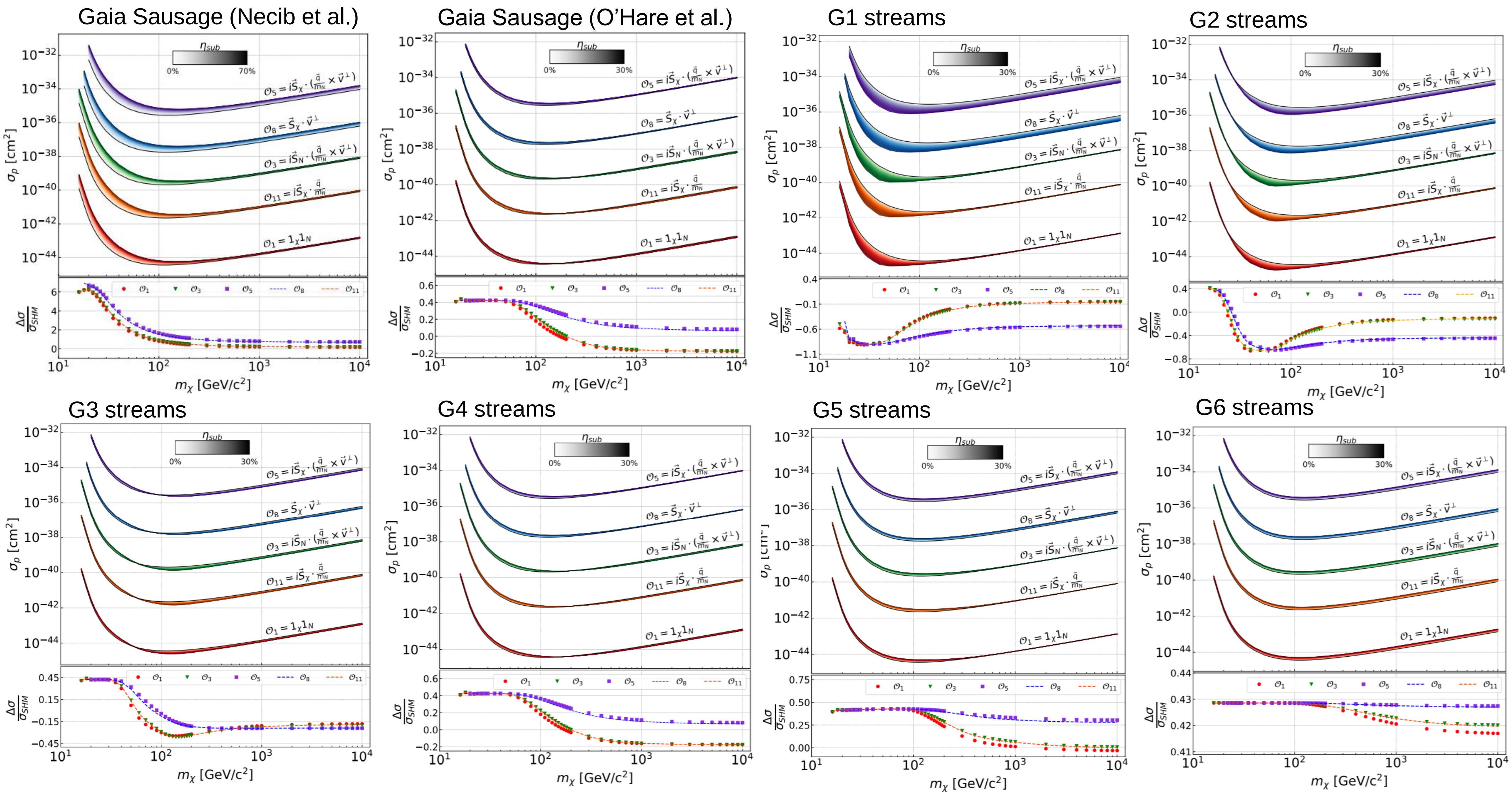

COMING SOON

- Blind Analysis of 3 years of data.
- Multivariate analysis for mitigation of alpha decays in the neck: Boosted Decision Trees, Random Forest and Convolutional Neural Networks.